ResearchGate

See discussions, stats, and author profiles for this publication at: https://www.researchgate.net/publication/299367691

High throughput P2 laser scribing of Cu(In,Ga)Se2 thin-film solar cells.

CONFERENCE PAPER · MARCH 2016

DOI: 10.1117/12.2212496

READS

2

9 AUTHORS, INCLUDING:

Andreas Burn

Bern University of Applied Sciences

9 PUBLICATIONS **33** CITATIONS

SEE PROFILE

Valerio Romano

Bern University of Applied Sciences and Univ…

130 PUBLICATIONS **1,902** CITATIONS

SEE PROFILE

All in-text references underlined in blue are linked to publications on ResearchGate, letting you access and read them immediately.

Available from: Andreas Burn
Retrieved on: 28 March 2016

High throughput P2 laser scribing of $Cu(In,Ga)Se_2$ thin-film solar cells

Andreas Burn[a,*], Christian Heger[a], Stephan Buecheler[b], Shiro Nishiwaki[b], David Bremaud[c], Roger Ziltener[c], Lukas Krainer[d], Gabriel Spuehler[d], Valerio Romano[a]

[a]Bern University of Applied Sciences, ALPS - Applied Laser-, Photonics- and Surface Technologies, Pestalozzistrasse 20, 3400 Burgdorf, Switzerland; [b]Laboratory for Thin Films and Photovoltaics, Empa, Swiss Federal Laboratories for Materials Science and Technology, Duebendorf, Switzerland; [c]Flisom AG, Ueberlandstrasse 129, 8600 Duebendorf, Switzerland; [d]Onefive GmbH, Althardstrasse 70, 8105 Regensdorf, Switzerland

ABSTRACT

Laser scribing is an indispensable step in the industrial production of $Cu(In,Ga)Se_2$ thin film solar modules. While cell separation (P1 and P3) is usually achieved using high velocity, low overlap lift-off processes, removal of the absorber layer for generating an electrical back-to-front interconnect (P2) is typically a slow process. In the present study we present an approach for scaling the classical P2 process velocity to an industrially exploitable level. We demonstrated successful P2 scribing at up to 1.7 m/s in a single beam, single pass configuration using a linear focal spot. The presented process is robust against variations in the scribing velocity and focal position, a key point for successful machine integration.

Keywords: laser scribing, CIGS, solar cell patterning, selective ablation, thin-film structuring, high throughput, process scaling, APPOLO

1. INTRODUCTION

Laser scribing is replacing traditional mechanical scribing in the production of $Cu(In,Ga)Se_2$ (CIGS) thin-film solar modules on all substrates. It is indispensable for patterning modules on flexible substrate such as polyimide in a roll-to-roll production line. In an in-line production setup the laser scribing sub-unit should preferably operate at the same throughput as the deposition machines in order to facilitate integration. For a typical industrial production scenario a scribing velocity of meters per second should preferably be achieved. In earlier studies [1, 2] we investigated various scribing process combinations and found optimum module performance when ultrashort pulsed lasers with pulse durations of tens of picoseconds were used. An efficiency of 16.6 percent (illuminated aperture) for an all-laser scribed mini module on 50x50 mm^2 float glass substrate was demonstrated [3]. The laser source used to realize said modules was the Katana HP fiber laser (Onefive GmbH, Switzerland) with maximum pulse energy of 15 µJ at 1064 nm. Scribing velocities for the three scribing processes were 50 mm/s for the P2 process (removal of the CIGS absorber layer and exposure of the molybdenum back contact) and 600 mm/s and 1200 mm/s for the P1 (isolation of the back contact) and P3 (selective removal of the front contact) process, respectively.

While low overlap P1 and P3 process can be scaled by increasing the pulse repetition frequency of the laser and changing the scribing velocity accordingly, P2 is not scalable with the same approach due to thermal relaxation of the material which has to be taken into account. As a result, published scribing velocities are rarely exceeding 200 mm/s [4, 5]. Alternative "non-classical" P2 processes were proposed, namely by Westin (thermal transformation of CIGS) [6] and Rekow (CIGS lift-off) [7], which follow different scaling laws. A comparative study of different P2 processes will be presented in a follow-up publication. Here we focus on the classical direct ablation process, which in our experiments up to now resulted in the best module performance.

* andreas.burn@bfh.ch; phone: +41 34 426 4246

Laser Applications in Microelectronic and Optoelectronic Manufacturing (LAMOM) XXI, edited by Beat Neuenschwander, Stephan Roth, Costas P. Grigoropoulos, Tetsuya Makimura, Proc. of SPIE Vol. 9735, 973504 · © 2016 SPIE · CCC code: 0277-786X/16/$18 · doi: 10.1117/12.2212496

2. SCALING OF THE CLASSICAL P2 SCRIBING PROCESS

2.1 Typical production scenario

For the development of a suitable high-throughput P2 scribing process a scenario needs to be defined first. In the present study we started from a typical roll-to-roll production machine. The roll width is 500 mm, the production speed 1-2 m/min and the height of the individual cell is 5-10 mm. Further, we assume cross-web scribing (scribe direction is perpendicular to the direction of the substrate movement) and in-line laser processing (one scribing unit per production machine). For this scenario the necessary net scribing velocity is in the range of 1-2 m/s. Departing from our reference P2 scribing process for 10 ps pulses at 1064 nm, where 0.3 W (3 µJ, 100 kHz, 50 ps) of average power were used for best quality scribing at 66 mm/s, a naïve process scaling (assuming no heat accumulation problems and no loss in optics) would predict 4.5 W average power necessary per m/s scribing velocity.

2.2 Heat accumulation problems

Increasing the pulse repetition frequency of the scribing laser is probably the first approach that comes to one's mind if the process velocity should be increased. Keeping pulse energy, pulse-to-pulse overlap and spot diameter constant, an increase in repetition frequency should lead to a proportional increase of the scribing velocity. It turns out that this reasoning is only correct for pulse repetition frequencies up to about 50 kHz. Between 50 kHz and 200 kHz heat accumulation starts to become increasingly significant and melting of the CIGS is observed. Working P2 processes can still be found but the stable parameter windows become smaller with increasing repetition frequency. Excessive melting destroys the selectivity of the ablation process. If damage of the molybdenum back contact occurs before the back contact is fully exposed the scribing process fails.
Interestingly, at repetition frequencies above 100 kHz, the highest working process velocities (around 200 mm/s) were found for increased fluence levels compared to the process at 50 kHz. The lower total number of thermal cycles seems to compensate for the increased amount of energy received per pulse. This is illustrated in Figure 1, where the scribes produced by three P2 process parameter sets at different pulse repetition frequencies are presented. The sample material ZnO/CdS/CIGS/Mo on glass substrate was produced by Empa. The described behavior is not limited to picosecond pulses but can also be observed for sub-picosecond pulses as shown in Figure 2 (same sample material); with an offset in necessary fluence and achieved translational velocity.

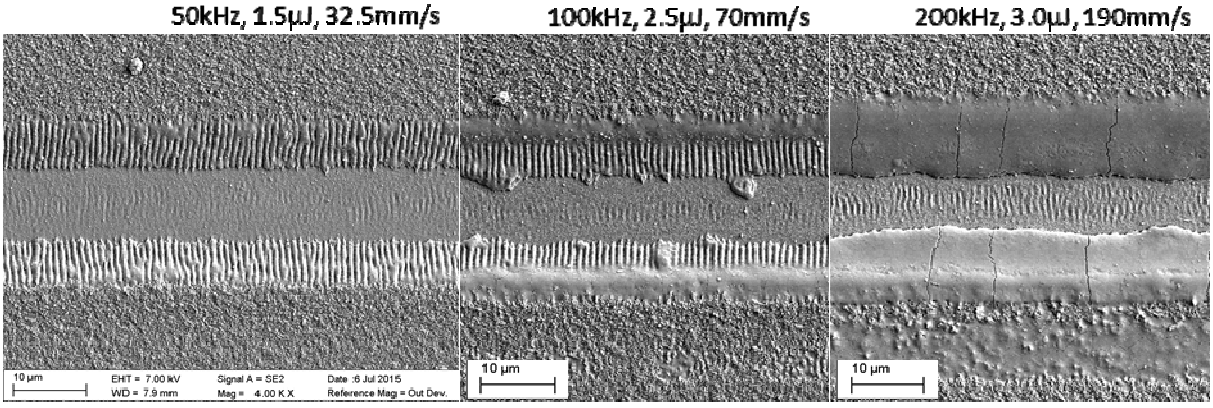

Figure 1 Three P2 scribes made with the same beam parameters but different pulse repetition frequency and pulse energy. Laser source used was an EKSPLA Atlantic 60W with emission at 1064 nm and pulse duration of 10 ps. The beam waist diameter was 24 µm (Gaussian, $1/e^2$) for all three cases. Fluence applied was 0.33 J/cm^2, 0.55 J/cm^2 and 0.66 J/cm^2. The melting below the scribe was caused by a satellite beam discovered later.

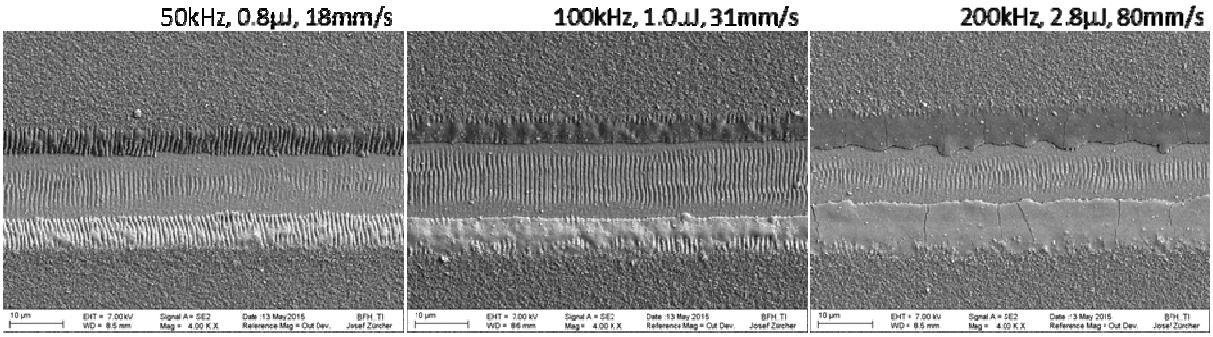

Figure 2 Three P2 scribes made with the same beam parameters but different pulse repetition frequency and pulse energy. Laser source used was an Origami XP, (Onefive GmbH, Switzerland) with emission at 1030 nm and pulse duration < 400 fs. The beam waist diameter was 28 µm (Gaussian, $1/e^2$) for all three cases. Fluence applied was 0.13 J/cm^2, 0.16 J/cm^2 and 0.45 J/cm^2.

Above a pulse repetition frequency of 200 kHz no viable and stable process was found at relevant scribing velocities. The before described behavior was equally observed for R&D samples produced by Empa on glass substrate as well as for commercial grade samples on flexible polyimide substrate manufactured by Flisom. On polyimide substrate heat accumulation is even more critical due to the less efficient heat extraction compared to glass. Similar observations were made by other research groups working on sample material from different producers [8]. No such heat accumulation problems were reported by Heise *et al.* [9, 10] who demonstrated P2 scribing at 1 m/s and 4 m/s, respectively without any additional measures using 10 ps pulses. It seems that the sample material used in the before cited studies differs from our samples in some specific properties promoting faster scribing. Since optimization of the material for scribing is usually not within the scope of cell manufacturers other strategies aimed at increasing P2 scribing velocities up to an industrially exploitable level need to be found. Some working approaches are described in the following section.

2.3 Multi pass approach

With the advent of fast scanning devices like high-end galvanometric or polygon scanners (e.g. from Next Scan Technology, Belgium) it is possible to circumvent heat accumulation problems by replacing the single-pass, high overlap scribing process by a multi-pass, low overlap process as shown in Figure 3. The effective application of pulse interleaving strategies has been demonstrated e.g. by Gečys *et. al*.[11]. In this way scribing velocities of several meters per second can be realized with pulse repetition frequencies in the MHz range and 10-20 passes per scribe. This approach is very attractive due to its simple working principle and easy process scalability (the same beam and laser parameters can be used except for the increased pulse repetition frequency and thus average power). There are, however, also some draw-backs which narrow the field of suitable applications in scribing. The scan length (of a polygon scanner) is fixed and typically shorter than the width of commercial substrate rolls. To realize multiple passes at the same position the sample has to stop until the scribe is complete or it has to move with the sample. Finally, the effectiveness of pulse interleaving for reducing accumulated heat depends on the scribe length.

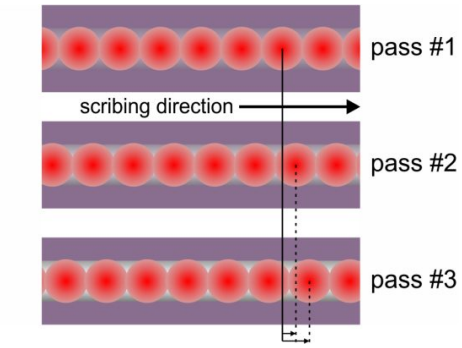

Figure 3 Illustration of the multi-pass "pulse interleaving" strategy. Starting from a standard P2 process where every point on the scribe is hit by n pulses the multi-pass P2 scribe is decomposed into n passes where only every n^{th} pulse is applied (pulse interleaving). Between the passes an offset of 1/(n+1) beam diameter is introduced.

2.4 Multi spot approach

A straight forward scaling approach is parallelization of the process by multiplication of the optical beam path and energy sharing between the simultaneous process sites (Figure 4). While the concept is simple in theory its realization may lead to rather complex optical systems that are difficult to align within acceptable tolerances. Splitting of the beam is possible using diffractive optical elements[12] or partially reflective mirrors. In both cases the challenge is to assure equidistant positioning of the spots, equal partition of the energy and equal beam parameters in each spot. Obviously, the alignment becomes more and more complex with the number of beam paths. In our scenario about 8 beamlines would be necessary. Further, variations in spot separation or change of scribing direction are not easily achieved.

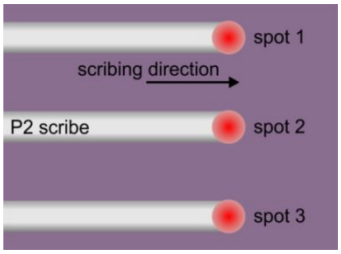

Figure 4 Illustration of a multi-spot parallelization approach for increasing P2 scribing speed.

2.5 Process area scaling approach

In our approach the advantages of multi-pass and multi-spot strategy are combined in the sense that a high-throughput scribe is achieved in a single pass, using a single beam path at low pulse repetition frequency. A high energy pulse is not discretely split into different spots but its energy is distributed homogeneously over a conjunct process area as shown in Figure 5 – hence the term "process area scaling". The distribution which has shown good process stability is a line focus with a flat top profile in direction of the line and a Gaussian-like profile in transversal direction.

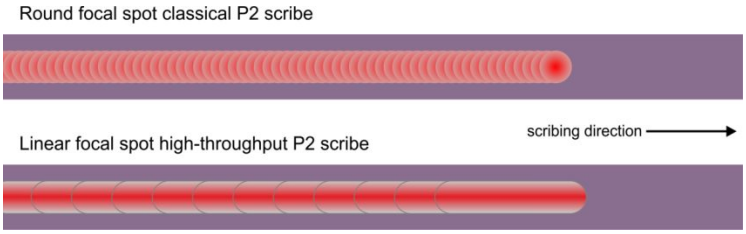

Figure 5 Illustration of the process area scaling approach. Pulse-to-pulse overlap is held constant as well as average fluence and pulse repetition frequency. With the chosen line geometry this results in an increase in scribing velocity proportional to the line length.

3. EXPERIMENTAL SETUP

3.1 Optical realization

The linear shape of the focus line element as shown in Figure 7 was achieved using a refractive beam shaper lens (e.g. GTH-4-2.2 from TOPAG, Germany) which, in conjunction with a spherical focusing lens, re-maps the Gaussian intensity distribution into a square flat top profile. Additional focusing by a cylindrical lens generates a linear focal spot with transversal Gaussian profile. The spot geometry can be adjusted within some limits by choosing focal length of spherical and cylindrical lens accordingly. Using this method, the full energy of the laser pulse can be used for scribing by choosing the geometrical shape (the aspect ratio) of the laser spot according to the necessary fluence and available pulse energy. In this configuration the achievable gain in scribing velocity is proportional to the pulse energy of the laser source. According to the chosen scenario which demands scribing velocities up to 2 m/s, linear spots with aspect ratio in the range of 20 to 30 were realized using the described method. Typically, the length of the linear spot was around 1.5 mm and the width ($1/e^2$) around 65 µm. A sample profile is shown in Figure 7 in a graphical representation. Exact geometries for three setups are given later in Table 1. Homogeneity of the peak intensity better than ±5 percent was regularly achieved in different setups.

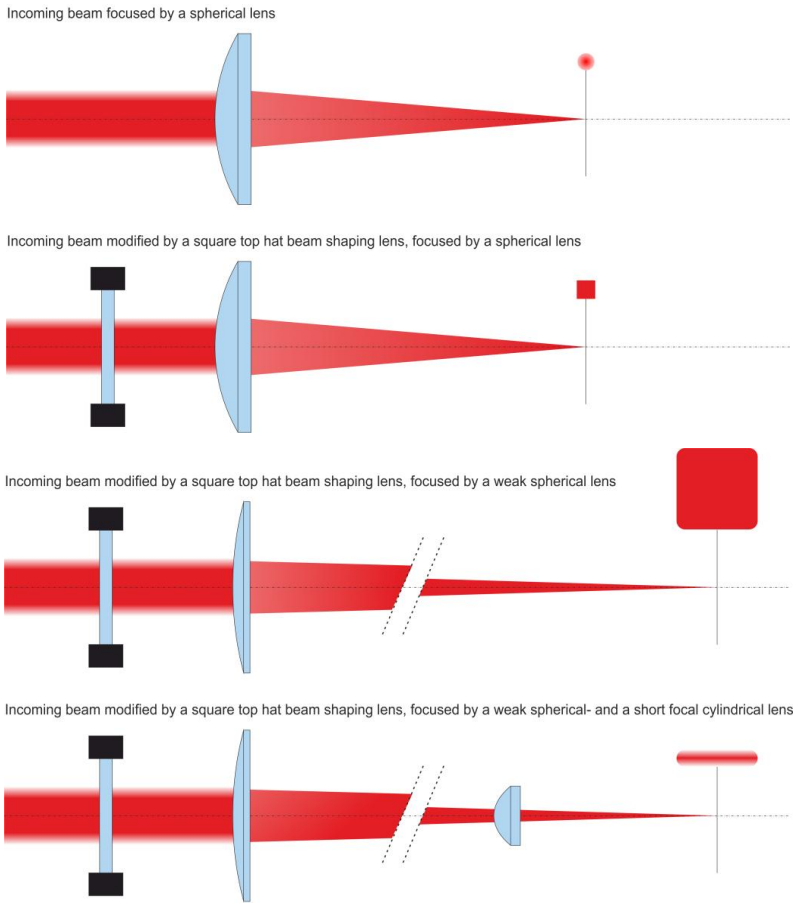

Figure 6 Line generation using a refractive flat-top beam shaping lens in combination with spherical and cylindrical lenses. Selection of linear spot width and aspect ratio is achieved by choosing focal lengths of the lenses accordingly.

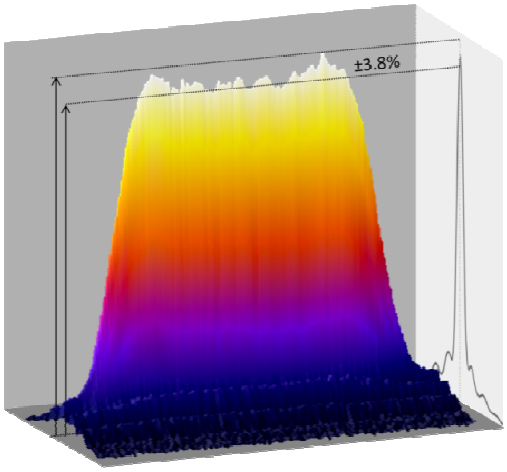

Figure 7 Graphical representation of a medium length flat top linear spot intensity profile recorded using a WinCAM D (DataRay Inc., Redding, USA). A variation in the peak intensity of less than ±5 percent was easily achieved.

3.2 Sample material

Samples used for P2 scribing tests were produced by Empa (R&D samples on float glas substrate) and Flisom AG (production samples on flexible polyimide substrate). In the case of the samples on glass substrate the thin-film stack was processed up to the intrinsic ZnO layer (glass/Mo/Cu(In,Ga)Se_2/CdS/ZnO) using Empa's own low-temperature (<500°C) multistage co-evaporation process with NaF post deposition treatment [13]. In the case of the samples on flexible substrate, Flisom full stack production samples were used and the ZnO:Al front contact was removed shortly before the experiments using a layer-selective laser stripping process.

3.3 Experimental procedure

Two ultrashort pulsed laser sources with different average power were used in the experiments. The first laser was a Genki XP from Onefive GmbH, Regensdorf, Switzerland, the second laser source was an EKSPLA Atlantic 60W manufactured by EKSPLA, Vilnius, Lithuania. Both lasers emit at 1064 nm and deliver pulses with pulse duration of approximately 10 ps. The maximum pulse energy for the two systems was 400 µJ for the Genki XP and 160 µJ for the Atlantic 60W (measured at the laser output). Both lasers were installed on a fully computer controlled lab scribing machine at BUAS based on X-Y linear axes as shown in Figure 8. Several focal spot geometries were realized following the approach described before. Dimensions of the linear focal spot and resulting exposed back contact width are listed in Table 1.

Figure 8 Lab scribing machine with optical experimentation platform installed at BUAS application lab.

Table 1 Geometry of the line focus elements used for high throughput P2 processing on glass and polyimide substrate.

	Onefive Genki XP on polyimide substrate	Onefive Genki XP on glass substrate	EKSPLA Atlantic 60W on glass substrate
focus line length ($1/e^2$)	1740 µm	1610 µm	1600 µm
focus line width ($1/e^2$)	63 µm	69 µm	58 µm
ablated line length	1560 µm	1450 µm	1440 µm
ablated line width	47 µm	56 µm	50 µm
exposed Mo length	1330 µm	1200 µm	1170 µm
exposed Mo width	20 µm	28 µm	24 µm

4. RESULTS

4.1 Scribe morphology

Scribe morphology was investigated using optical microscopy, scanning electron microscopy (SEM) and laser scanning microscopy (LSM). Optical microscopy was used as a first feedback on the scribing result during parameter study and for gathering color-related information such as a color transformation in the heat affected zone (HAZ). LSM helped to exclude substantial ablation of the back contact. SEM was predominantly used for identification and qualification of micro-cracks, to detect beginning delamination (in tilted mode) and for the analysis of melt formation under different process conditions. Some SEM images illustrating some very pronounced scribe failures for different damage mechanisms are presented in Figure 9.

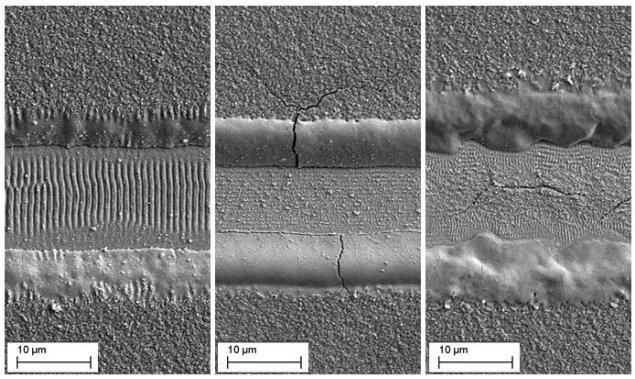

Figure 9 Three examples of often observed problems in P2 scribing (left to right): damage of the back contact layer (by strong ripple formation or ablation of the back contact), micro-cracks extending into the surrounding absorber material with beginning delamination of the layer stack, and cracks in the back contact in the direction of the scribe (thermal overload caused by heat accumulation).

SEM images in the following section show typical scribing results for the three high throughput processes investigated in this study. For comparison, a conventional scribe is depicted in Figure 10. This image shows a typical situation for a scribe optimized for integrity of the back contact, minimal melt and small heat affected zone. Also typical for such a scribe is the slow scribing velocity achieved – 32.5 mm/s in this case.

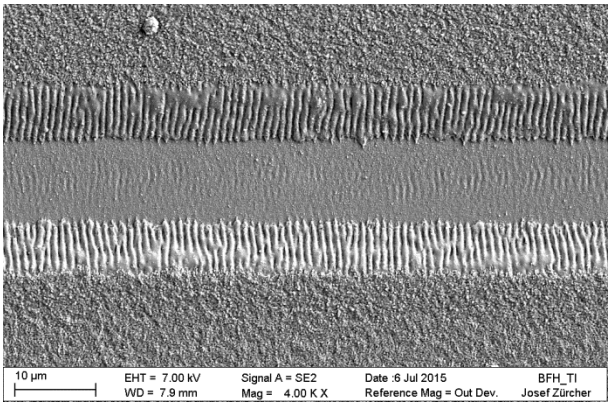

Figure 10 Electron micrograph of a P2 scribe realized on glass substrate using a conventional round focal spot with Gaussian intensity profile. The process parameters used in this example were: pulse energy 1.5 µJ, repetition frequency 50 kHz, scribing velocity 32.5 mm/s; the laser source used was the EKSPLA Atlantic 60W emitting 10 ps pulses at 1064 nm.

Figure 11 shows a high-throughput P2 scribe realized on polyimide substrate using the proposed area-scaling approach and a linear focal spot, the laser source used was the Onefive Genki XP at 250 µJ and 10 kHz pulse repetition frequency. The scribe image shows a clean and damage free exposure of the back contact, virtually no micro-cracks and low melting. Note that the slight change in surrounding CIGS surface structure results from stripping of the front contact described in 3.2. In this experiment not the full available laser pulse energy of 400 µJ was used. A proper optimization of the linear focus aspect ratio was not possible in this case due to time constraints. For an optimized linear spot a scribing velocity in excess of 600 mm/s can be expected at 400 µJ and 10 kHz pulse repetition frequency.

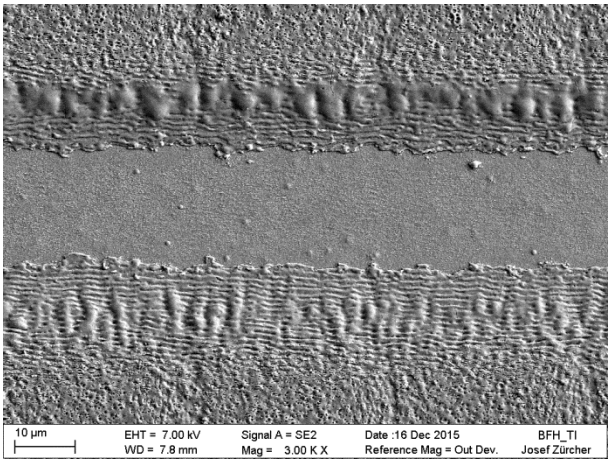

Figure 11 P2 scribe realized on flexible substrate (Mo/CIGS on PI substrate; Flisom). The laser used was Onefive Genki XP at 2.5 W average power and a wavelength of 1064 nm. Achieved scribing velocity: 380 mm/s.

Figure 12 shows a P2 scribe realized on glass substrate using the Onefive Genki XP at 400 µJ pulse energy and 10 kHz pulse repetition frequency. The scribe image shows a clean exposure of the back contact with marginal ripple formation in the molybdenum. Micro-cracks in the CIGS and melting are not observed. The process is limited by the available laser power only. Further scaling of the scribing velocity by increasing the pulse repetition frequency at constant pulse energy seems possible.

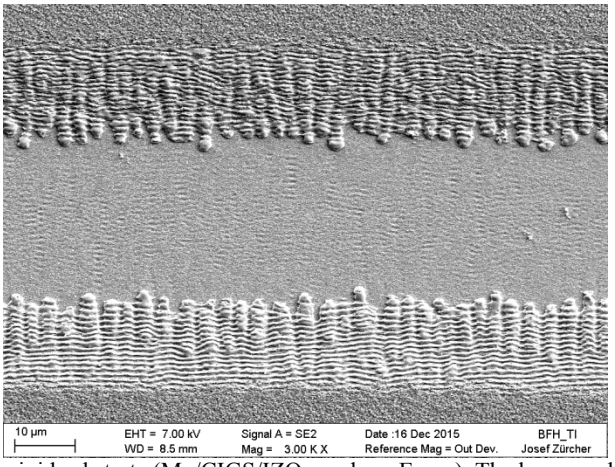

Figure 12 P2 scribe realized on rigid substrate (Mo/CIGS/IZO on glass; Empa). The laser used was Onefive Genki XP at around 4 W average power and a wavelength of 1064 nm. Achieved scribing velocity: 390 mm/s.

Further scalability of the process was demonstrated using the EKSPLA Atlantic 60W laser with comparable pulse characteristics but higher average power. This source delivers constant pulse energy of 160 µJ up to the 400 kHz pulse repetition frequency of the master oscillator. A successful scaling of the high-throughput P2 scribing process up to a scribing velocity of 1720 mm/s was demonstrated (see Figure 13). In this experiment a pulse repetition frequency up to 67 kHz was used. As the scribe image in Figure 13 shows, heat accumulation leads to melting of the remaining CIGS material. Local micro-cracks are observed which do not extend into the unprocessed material. Some droplets of molten CIGS were deposited on the exposed molybdenum layer during the process. Nevertheless, the back contact was not damaged and the exposed area is large enough for a good electrical contact. In this experiment the achievable scribing velocity was limited by two factors; on the one hand by the mechanical axes whose velocity is limited to 2 m/s and on the other hand by the available laser pulse energy. A further scaling of the process seems possible if pulse energy and focal line length are increased. At 400 µJ pulse energy and 67 kHz repetition frequency a scribing velocity in excess of 4 m/s can be expected. Since this velocity level is beyond the scope of our scenario of industrial application and beyond the capabilities of our hardware we did not further investigate practical scaling realization at these velocity levels.

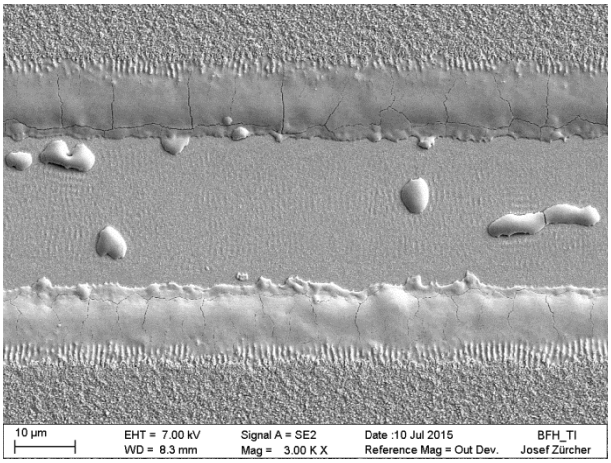

Figure 13 P2 scribe realized on rigid substrate (Mo/CIGS/IZO on glass; Empa). The laser used was the EKSPLA Atlantic 60W at around 11 W average power and a wavelength of 1064 nm. Achieved scribing velocity: 1720 mm/s.

4.2 Process robustness

The proposed high-throughput P2 process was found to be extremely robust with respect to variations in the scribing speed and position of the focal plane. The process shown in Figure 12 did produce almost identical results when the scribing velocity was varied between 350 mm/s and 425 mm/s as shown in Figure 14. This result demonstrates a high tolerance against fluctuations in the translational velocity of the linear scribing axis which allows the use of lower cost components. Even more important for the integration of a laser process in a roll-to-roll production machine is the tolerance with respect to the focal position. The top hat generator, which is based on a refractive design, and the long focal length of the spherical lens create a large square top hat beam whose shape and size varies only marginally when moving along the optical axis. In the case where the cylindrical lens is installed as well, the divergence of the beam in direction of the focus line is approximately 10 times smaller than perpendicular to the line. Compared to a symmetrical Gaussian beam where the power density at one Rayleigh range drops to $\frac{1}{2}$ of the value in the focal plane, the power density in the case of a linear focal spot drops only to approximately $\frac{1}{\sqrt{2}}$ of the maximum value. This leads to an extraordinary large operating z-range of several millimeters as demonstrated in Figure 15.

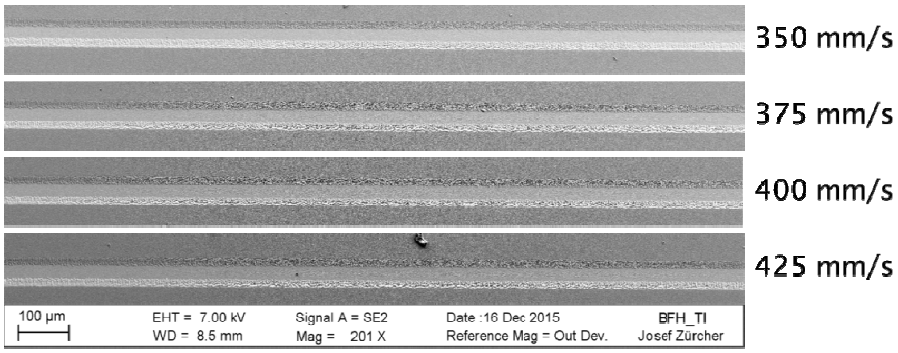

Figure 14 Four P2 scribes realized at identical laser parameters but different scribing velocities. The SEM images show no significant difference between the scribes. Genki XP on glass substrate, 4 W@10 kHz

Figure 15 Robustness of the high-throughput P2 process with respect to changes of the focal position. Between scribing of each of the lines the focal position was shifted by 1 mm. All but the leftmost scribe show successful removal of the CIGS without Mo damage and thus valid P2 scribes.

4.3 Process efficiency

Based on used scribing parameters and resulting scribe geometry, efficiency figures can be calculated to compare different scribing processes. One measure of process efficiency is the necessary total laser pulse energy per unit length of the scribe (which is equivalent to the necessary laser power at 1 m/s). If the width of the scribe is also considered, the total applied pulse energy can be related to the area of the exposed back contact. The described efficiency figures calculated for the three investigated high-throughput classical P2 processes (employing line focus) and a reference scribe made with the EKSPLA Atlantic 60W using a round Gaussian spot with a diameter of 22 µm ($1/e^2$) are listed in Table 2. Due to the significant differences in scribe geometry a direct comparison of values listed for the individual processes is difficult. However, if the width of the exposed back contact trench is taken into account, the energy necessary for exposing an area of 1 mm^2 of the molybdenum back is roughly 300 mJ in all our investigated P2 processes. In this sense the process efficiency of the high throughput classical P2 process using a linear spot is comparable to the one of the reference process using a round Gaussian spot. A further common characteristic is the high overlap between 97 percent and 98 percent for all processes.

Table 2 Laser and motion parameters used for high throughput P2 processing on glass and polyimide substrates and corresponding process efficiency figures.

	Onefive Genki XP on polyimide substrate	Onefive Genki XP on glass substrate	EKSPLA Atlantic, glass substrate	EKSPLA round spot on glass
laser pulse energy	250 µJ	400 µJ	160 µJ	1.5 µJ
approx. average fluence(*)	0.23 J/cm^2	0.26 J/cm^2	0.18 J/cm^2	0.4 J/cm^2
pulse repetition frequency	10 kHz	10 kHz	67 kHz	50 kHz
scribing velocity	380 mm/s	390 mm/s	1720 mm/s	32.5 mm/s
energy per scribe length unit	66 mJ/cm	103 mJ/cm	62 mJ/cm	23 mJ/cm
energy per exposed Mo area	330 mJ/mm^2	366 mJ/mm^2	260 mJ/mm^2	320 mJ/mm^2
laser power needed @1 m/s	6.6 W	10.3 W	6.2 W	2.3 W

(*) The average fluence was approximated as pulse energy divided by the area of the linear spot. The spot area was determined from a grey-level image of the intensity profile with threshold set at $1/e^2$ of the maximum intensity.

4.4 Electrical quality

Direct electrical testing of P2 scribe contact resistance has played an important role during development and optimization of the high throughput process. For this purpose, test structures have been produced for direct comparison of different P2 scribes. The simplified test structure allowed measuring cumulative resistance of front contact, back contact and contact resistance of the P2 scribe for many P2 process variants on one sample. In these tests high-throughput processes did

show similar electrical properties as the reference process. Currently, selected high-throughput P2 processes are validated in functional modules and test structures allowing us to extract specific data for the P2 contact resistance. The result of these measurements will be published as a comparative study in a follow-up publication.

5. CONCLUSION AND OUTLOOK

In the present study different scaling approaches for P2 scribing were investigated for an industrial scenario demanding 1-2 m/s scribing velocity. A simple and effective "process area scaling" approach was proposed employing a linear focus element and high energy ultrashort laser pulses. The optical realization is simple and low-cost, based only on refractive optics. The process is extraordinarily robust against variations in scribing velocity and the z-position of the sample, therefore it is ideally suited to be used on a roll-to-roll production machine where maintaining a constant z-position of the flexible substrate is challenging. In scribing experiments good scribe quality was achieved with minimal substrate damage and no delamination. Scalability of the process up to a scribing velocity of 1720 mm/s was demonstrated and further scaling is possible if necessary using high energy, low repetition frequency ultrashort pulsed laser sources. Together with the low overlap and high throughput P1 and P3 processes a full set of industrially exploitable laser scribing processes is now available. In-depth characterization and validation of the scribing processes is currently running and will be one of the outcomes of the FP7 project APPOLO.

ACKNOWLEDGEMENTS

The present study was conducted in the frame of the collaborative project APPOLO funded under EC Grant Agreement N° 609355 in the 7th Framework Programme. www.appolo-fp7.eu
We would like to thank Josef Zürcher at Bern University of Applied Sciences for the preparation of SEM images.

REFERENCES

[1] A. Burn, V. Romano, M. Muralt *et al.*, “Selective ablation of thin films in latest generation CIGS solar cells with picosecond pulses,” SPIE LASE, 8243, 824318-17 (2012).
[2] A. Burn, M. Muralt, S. Pilz *et al.*, “All Fiber Laser Scribing of Cu(In,Ga)Se2 Thin-Film Solar Modules,” Physics Procedia, 41, 713-722 (2013).
[3] S. Nishiwaki, A. Burn, S. Buecheler *et al.*, “A monolithically integrated high-efficiency Cu(In,Ga)Se2 mini-module structured solely by laser,” Progress in Photovoltaics: Research and Applications, 23(12), 1908-1915 (2015).
[4] G. Račiukaitis, E. Stankevičius, P. Gečys *et al.*, “Laser Processing by Using Diffractive Optical Laser Beam Shaping,” JLMN-Journal of Laser Micro/Nanoengineering, 6(1), (2011).
[5] D. Ruthe, K. Zimmer, and T. Höche, “Etching of CuInSe2 thin films—comparison of femtosecond and picosecond laser ablation,” Applied Surface Science, 247(1–4), 447-452 (2005).
[6] P. O. Westin, U. Zimmermann, and M. Edoff, “Laser patterning of P2 interconnect via in thin-film CIGS PV modules,” Solar Energy Materials and Solar Cells, 92(10), 1230-1235 (2008).
[7] M. Rekow, R. Murison, C. Dunsky *et al.*, "CIGS P1, P2, P3 scribing processes using a pulse programmable industrial fiber laser." 2862-2871 (2010).
[8] A. Lemke, D. Ashkenasi, and H. J. Eichler, “Picosecond Laser Induced Selective Removal of Functional Layers on CIGS Thin Film Solar Cells,” Physics Procedia, 41, 769-775 (2013).
[9] G. Heise, M. Domke, J. Konrad *et al.*, “Monolithical Serial Interconnects of Large CIS Solar Cells with Picosecond Laser Pulses,” Physics Procedia, 12, Part B, 149-155 (2011).
[10] G. Heise, A. Börner, M. Dickmann *et al.*, “Demonstration of the monolithic interconnection on CIS solar cells by picosecond laser structuring on 30 by 30 cm2 modules,” Progress in Photovoltaics: Research and Applications, 23(10), 1291-1304 (2015).

[11] P. Gečys, G. Račiukaitis, M. Ehrhardt *et al.*, "ps-laser scribing of CIGS films at different wavelengths," Applied Physics A, 101(2), 373-378 (2010).
[12] P. Gečys, G. Račiukaitis, E. Miltenis *et al.*, "Scribing of Thin-film Solar Cells with Picosecond Laser Pulses," Physics Procedia, 12, Part B, 141-148 (2011).
[13] A. Chirilă, S. Buecheler, F. Pianezzi *et al.*, "Highly efficient Cu(In,Ga)Se2 solar cells grown on flexible polymer films," Nat Mater, 10(11), 857-861 (2011).